

# Differential Shunting of EPSPs by Action Potentials

Michael Häusser,<sup>1\*</sup>† Guy Major,<sup>2‡</sup> Greg J. Stuart<sup>3\*\*</sup>

Neurons encode information and communicate via action potentials, which are generated following the summation of synaptic events. It is commonly assumed that action potentials reset the membrane potential completely, allowing another round of synaptic integration to begin. We show here that the conductances underlying the action potential act instead as a variable reset of synaptic integration. The strength of this reset is cell type-specific and depends on the kinetics, location, and timing of the synaptic input. As a consequence, distal synapses, as well as inputs mediated by *N*-methyl-D-aspartate receptor activation, can contribute disproportionately to synaptic integration during action potential firing.

Most neurons fire action potentials (APs) continuously in vivo. As a consequence, APs and synaptic potentials are constantly interacting during normal brain function. The pioneering work of Eccles and colleagues in spinal motor neurons (1, 2) suggested that APs can reset the membrane potential during an excitatory postsynaptic potential (EPSP), consistent with the large conductances underlying the AP (3). This “shunting” behavior of APs is incorporated into integrate-and-fire models of neurons, where APs typically generate a complete reset of synaptic integration (4). Most neurons, however, have extended dendritic trees and cannot be described by a single electrical compartment. Furthermore, recent experiments have demonstrated that different neurons express different voltage-gated channels (5), which are not uniformly distributed over the neuronal membrane (6). This raises the possibility that in different neurons and at different synapses, APs will shunt EPSPs to different extents.

To examine this possibility, APs were paired with EPSPs during whole-cell patch-clamp recordings from neocortical layer 5 pyramidal and cerebellar Purkinje neurons in rat brain slices (7). Subtraction of APs elicited in isolation from paired responses revealed that the EPSP remaining after the AP (the “shunted EPSP”) was greatly reduced both in peak amplitude and integral (Fig. 1A). The magnitude of this EPSP shunting depended on cell type. In pyramidal neurons, APs reduced EPSP amplitude to  $30 \pm 3\%$

( $n = 10$ ) of control EPSP amplitude at the same time point (8), whereas EPSPs in Purkinje neurons were reduced to only  $73 \pm 3\%$  of control (Fig. 1B;  $n = 7$ ;  $P < 0.05$ ). In both cell types, large ( $>6$  mV) and small EPSPs ( $<2$  mV) were shunted to a similar extent ( $P > 0.05$ ).

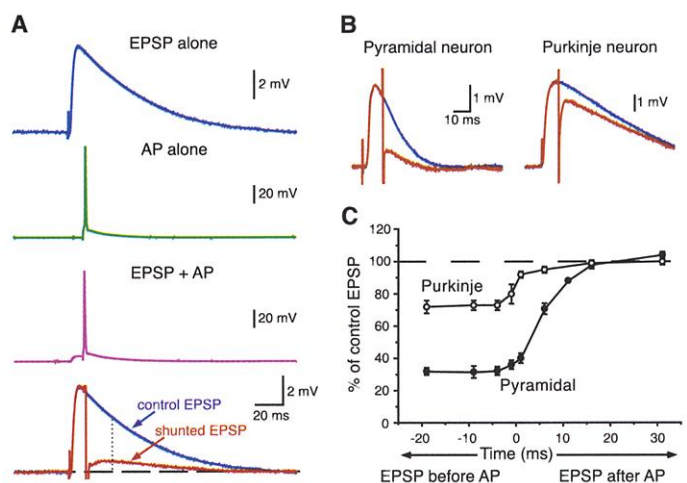
EPSP shunting was highly sensitive to the relative timing of the AP and the EPSP. Shunting was maximal when the AP was initiated after EPSP onset and absent when the AP occurred more than 15 ms before the EPSP (Fig. 1C) (9). These findings suggest that EPSP shunting is generated predominantly by the AP itself, rather than conductances activated during the after-hyperpolarization (AHP). Consistent with this, EPSP shunting was similar in pyramidal neurons recorded with a pipette solution containing 20 mM 1,2-bis(2-amino-phenoxy)ethane-*N,N,N',N'*-tetraacetic acid

(BAPTA) to block the calcium-dependent AHP (10) ( $26 \pm 12\%$  of control,  $n = 7$ ;  $P > 0.05$ ). To investigate whether shunting of EPSPs by APs is mediated by a change in driving force of the synaptic conductance, we mimicked EPSPs with somatic current injection (11). At times when the synaptic conductance should be active (AP onset 3 ms after EPSP onset), shunting of EPSPs generated by somatic current injection ( $30 \pm 5\%$  of control) was similar to that of evoked EPSPs ( $29 \pm 6\%$  of control,  $n = 4$ ;  $P > 0.05$ ). This indicates that the conductances underlying the AP, rather than changes in synaptic driving force, generate EPSP shunting.

Shunting of EPSPs generated by current injection depended strongly on the kinetics of the injected waveform, with EPSPs generated by using slow kinetics being shunted less than those generated by using fast kinetics (Fig. 2, A and B). Shunting of EPSPs generated by identical somatic current waveforms was always less in Purkinje neurons (Fig. 2B). This indicates that differences in EPSP shunting between pyramidal and Purkinje neurons (Fig. 1, B and C) are mediated by cell-specific differences in the AP rather than differences in excitatory postsynaptic current (EPSC) time course. In support of this idea, APs in neocortical pyramidal neurons are significantly broader than in Purkinje neurons (half-width  $0.39 \pm 0.02$  ms ( $n = 5$ ) versus  $0.15 \pm 0.01$  ms ( $n = 4$ );  $P < 0.001$ ).

The dependence of shunting on EPSC kinetics (Fig. 2B) suggests that EPSPs generated by transmitter-gated channels with slower kinetics will experience less shunting. Consistent with this idea, *N*-methyl-D-aspartate (NMDA) receptor-mediated EPSPs were shunted far less

**Fig. 1.** Shunting of EPSPs by APs. (A) Activation of an EPSP (top), an AP by a brief current pulse (2 ms, 1.4 nA; second from top), and concurrent activation of both EPSP and AP (second from bottom). The bottom panel shows the shunted EPSP (red), obtained by subtracting the AP from the trace where the EPSP and AP were evoked concurrently, together with the control EPSP evoked in isolation (blue). The dotted line indicates the time at which the amplitudes of the shunted and control EPSPs were compared. Averages of 10 to 15 interleaved trials recorded at the soma of a layer 5 pyramidal neuron ( $V_m = -60$  mV). (B) Control and shunted EPSPs in a layer 5 pyramidal neuron (left) and a Purkinje neuron (right). The EPSP preceded the antidromic AP by 10 ms. (C) Time window for shunting in layer 5 pyramidal and Purkinje neurons. Percentage reduction in shunted EPSP amplitude plotted against the time difference between EPSP and AP onset; positive times: AP precedes EPSP. Average from five to seven neurons.



<sup>1</sup>Department of Physiology, University College London, Gower Street, London WC1E 6BT, UK. <sup>2</sup>University Laboratory of Physiology, Parks Road, Oxford OX1 3PT, UK. <sup>3</sup>Division of Neuroscience, John Curtin School of Medical Research, Australian National University, Canberra, ACT 0200, Australia.

\*These authors contributed equally to this work.

†To whom correspondence should be addressed. E-mail: m.hauser@ucl.ac.uk

‡Present address: Bell Laboratories, Lucent Technologies, Murray Hill, NJ 07974, USA.

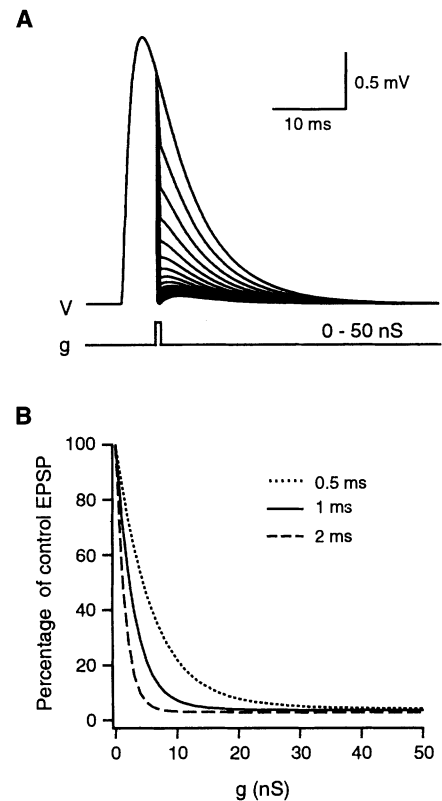
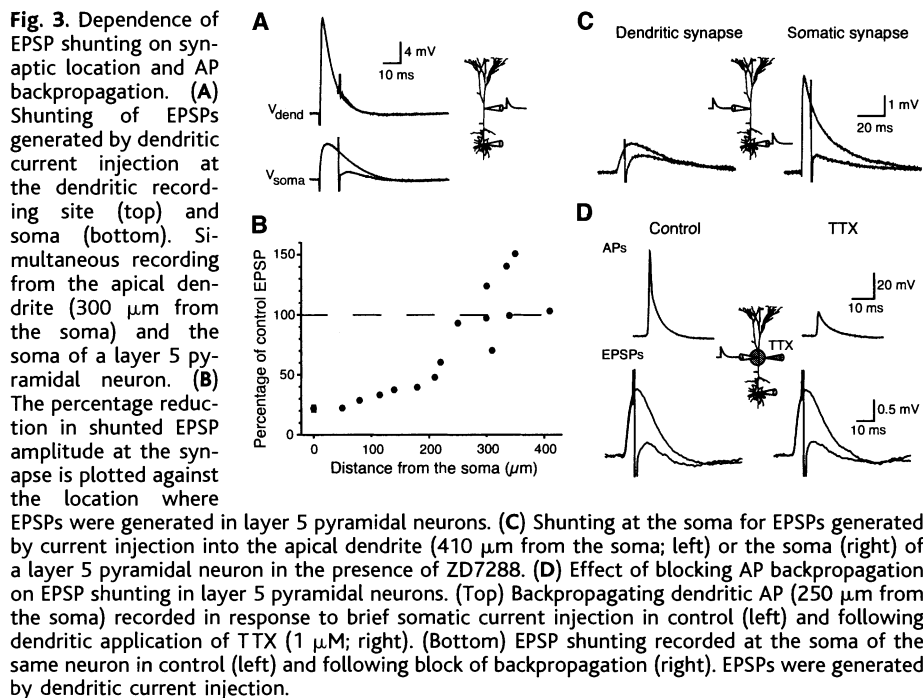
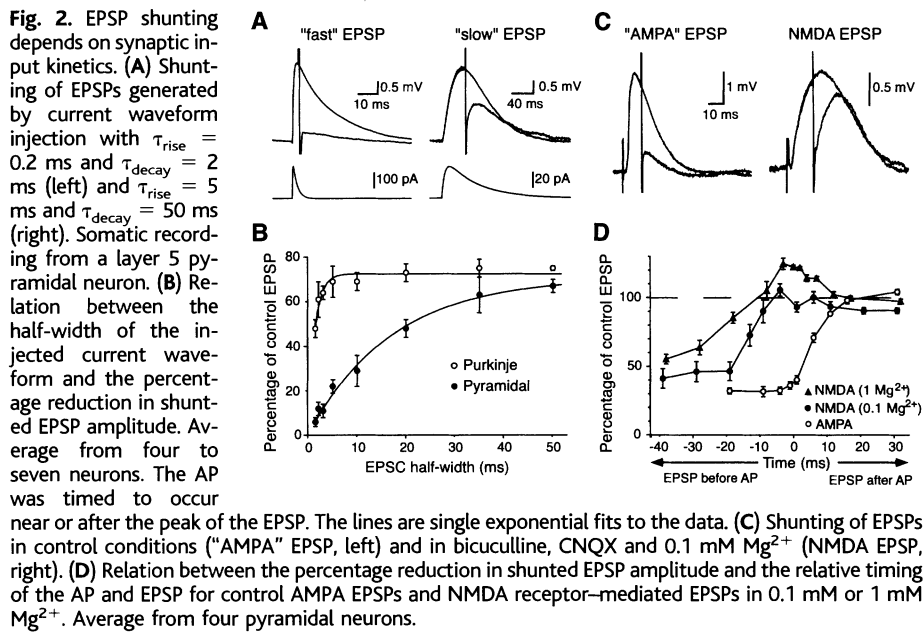
REPORTS

by APs timed at their peak ( $90 \pm 8\%$  of control;  $n = 8$ ) than EPSPs mediated by activation of  $\alpha$ -amino-3-hydroxy-5-methyl-4-isoxazolepropionate (AMPA)-type glutamate receptors (Fig. 2C;  $22 \pm 4\%$  of control;  $n = 6$ ). The relation between EPSP shunting and AP timing was also different for the two types of EPSPs. NMDA EPSPs evoked simultaneously with or after the AP experienced little or no shunting, whereas shunting similar to that for AMPA EPSPs was attained when APs were evoked more than 20 ms after NMDA EPSP onset (Fig. 2D). The difference between shunting of EPSPs mediated by AMPA and NMDA receptors was further

enhanced for NMDA EPSPs recorded in physiological concentrations of  $Mg^{2+}$  (1 mM), where relief of  $Mg^{2+}$  block (12, 13) could boost appropriately timed NMDA EPSPs (Fig. 2D).

Our finding that EPSP shunting is mediated primarily by the AP itself suggests that shunting may be greatest close to the soma, near the site of AP generation in the axon (14). We therefore generated EPSPs by current injection at different dendritic locations and examined shunting both at the site of EPSP origin and at the soma. The EPSP arriving at the soma was always shunted more than the EPSP at its site of generation in

the dendrites (Fig. 3A), with a clear relation between the magnitude of shunting at the site of EPSP generation and distance from the soma (Fig. 3B). This result indicates that shunting is relatively ineffective at distances greater than  $\sim 300 \mu\text{m}$  from the soma (Fig. 3, A and B). These experiments also allowed us to assess whether shunting of EPSPs at the soma depends on synaptic location (15). Indeed, somatically recorded EPSPs generated by dendritic current injection ( $408 \pm 17 \mu\text{m}$  from the soma,  $n = 5$ ) were shunted significantly less than those generated by current injection at the soma (Fig. 3C; somatic current injection  $33 \pm 4\%$  of control versus  $68 \pm 4\%$  for dendritic current injection;  $P < 0.005$ ) (16). To examine the contribution of dendritic conductances activated by backpropagating APs to EPSP shunting, we blocked backpropagation by dendritic application of tetrodotoxin (TTX) (Fig. 3D). At the soma, shunting of EPSPs generated by dendritic current injection ( $290 \pm 16 \mu\text{m}$  from the soma) was unchanged after application of TTX (control:  $24 \pm 5\%$ ; dendritic TTX:  $18 \pm 3\%$ ;  $n = 5$ ;  $P > 0.05$ ), despite a



57 ± 8% reduction in backpropagating AP amplitude at the site of EPSP generation (Fig. 3D) (17). These results indicate that conductances in the apical dendrite activated during backpropagating APs do not contribute significantly to EPSP shunting at the soma.

Simulations using neuronal models were used to gain more insight into the mechanisms of EPSP shunting by APs. Some key features of EPSP shunting could be reproduced in a single-compartment model (18) by using brief rectangular conductance pulses in the nanosiemens range to represent the AP (Fig. 4, A and B). Increasing the duration—and thus also the integral—of the conductance pulse increased the extent of EPSP shunting (Fig. 4B), consistent with the idea that differences in AP width underlie differences in EPSP shunting in pyramidal and Purkinje neurons (Fig. 1, B and C). We also observed shunting of EPSPs using realistic AP conductances in compartmental models with morphologically realistic geometries (19).

Finally, we examined the effect of EPSP shunting by APs on temporal summation at the soma of neocortical pyramidal neurons. EPSPs were generated by somatic current injection, and temporal summation of two EPSPs was quantified by measuring the peak current required for the second EPSP to reach AP threshold. These experiments revealed that when an AP occurred during the first EPSP, the efficacy

of the second input was similar to when the AP was evoked on its own (Fig. 5, A to D). This indicates that APs can significantly reduce temporal summation of EPSPs. Summation generated by EPSPs with slow current kinetics was less affected by an intervening AP ( $P < 0.05$ ), consistent with reduced shunting of slower EPSPs (Fig. 2). These results are summarized in Fig. 5E, and demonstrate that the effect of APs on temporal summation will depend on the extent to which they shunt coincident synaptic input.

Our findings provide a fresh perspective on the role of APs in synaptic integration. Rather than simply riding on top of EPSPs, the large conductances activated during the AP influence integration by rapidly shunting synaptic charge from the membrane. The reset of synaptic integration is not complete, however, as in classical integrate-and-fire models (4). Rather, a variable amount of synaptic charge survives each AP, depending on neuronal type, the relative timing of the AP and the synaptic input, and the kinetics and location of the synaptic conductance. As many neurons fire APs at high rates in vivo, integration will only take place over a narrow time window unless mechanisms are in place to mitigate shunting. It is noteworthy that Purkinje neurons fire at unusually high rates in

vivo [ $>50$  Hz (20)] and show much less shunting than pyramidal neurons, possibly because they have optimized their AP conductances to minimize shunting. Other neurons may achieve the same result by using slower synaptic conductances, such as those mediated by NMDA receptors (which Purkinje neurons lack). Finally, as distal inputs survive shunting, we predict that they will contribute disproportionately to synaptic integration during high levels of AP firing. By defining multiple spatial compartments and temporal windows for summation of synaptic inputs, shunting of synaptic potentials by APs represents a powerful computational mechanism influencing the way neurons integrate the many thousands of synaptic inputs they receive.

References and Notes

1. J. S. Coombs, J. C. Eccles, P. Fatt, *J. Physiol. (London)* **130**, 374 (1955).
2. D. R. Curtis, J. C. Eccles, *J. Physiol. (London)* **145**, 529 (1959).
3. K. S. Cole, H. J. Curtis, *J. Gen. Physiol.* **22**, 649 (1939).
4. C. Koch, *Biophysics of Computation* (Oxford Univ. Press, New York, 1999).
5. R. R. Llinás, *Science* **242**, 1654 (1988).
6. M. Häusser, N. Spruston, G. J. Stuart, *Science* **290**, 739 (2000).
7. Recordings were made from layer 5 pyramidal neurons from somatosensory cortex or from cerebellar Purkinje neurons in 300- $\mu$ m-thick sagittal slices from 3- to 4-week-old rats at  $35^\circ \pm 1^\circ$ C (27). The extracellular solution contained (in millimolar concentration): NaCl, 125; KCl, 2.5 or 3.0;  $\text{NaH}_2\text{PO}_4$ , 1.25;  $\text{NaHCO}_3$ , 25; glucose, 25;  $\text{CaCl}_2$ , 2;  $\text{MgCl}_2$ , 1; at pH 7.4. Pipettes were filled with internal solution containing (in millimolar concentration): K-gluconate, 135; Hepes, 10; EGTA, 0.1;  $\text{MgCl}_2$ , 2;  $\text{Na}_2\text{ATP}$ , 2; GTP, 0.3; KCl, 7; at pH 7.3. In some experiments, the K-gluconate concentration was lowered, and the EGTA concentration was raised to 1 or 10 mM; in others, EGTA was replaced by 20 mM BAPTA, which increased AP half-width from  $0.47 \pm 0.04$  ms to  $0.61 \pm 0.08$  ms as BAPTA diffused into the neuron. The APs were elicited by brief somatic current pulses (0.5 to 2 ms, 2 to 5 nA) or by axonal stimulation via a patch pipette filled with extracellular solution. These methods resulted in similar degrees of shunting in neocortical pyramidal neurons ( $21 \pm 2\%$  versus  $27 \pm 5\%$ ;  $n = 5$ ;  $P > 0.05$ ). EPSPs were evoked by extracellular stimulation in layer 5 or layer 2/3 in neocortical slices and in the molecular layer in cerebellar slices. In some cases, AMPA EPSPs were evoked in the presence of bicuculline (20  $\mu$ M) and D,L-2-amino-5-phosphonovaleic acid (APV, 50  $\mu$ M), whereas NMDA EPSPs were evoked in the presence of 6-cyano-7-nitroquinoxaline-2,3-dione (CNQX, 10  $\mu$ M), bicuculline (20  $\mu$ M), and 0.1 or 1 mM  $\text{Mg}^{2+}$ . All data are presented as means  $\pm$  SEM.
8. Shunting was quantified as the percentage change in the peak amplitude of the shunted EPSP after the AP relative to that of the control EPSP at the same time point. To assess the degree of shunting, the AP onset was timed to occur  $10 \pm 0.5$  ms after EPSP onset, unless otherwise indicated.
9. The shape of the timing curve was similar for the peak and integral of the shunted EPSP.
10. J. F. Storm, *Brain Res.* **435**, 387 (1987).
11. The EPSPs were mimicked by injecting current waveforms via somatic or dendritic recording pipettes. The kinetics of the standard waveform was  $\tau_{\text{rise}} = 0.3$  ms and  $\tau_{\text{decay}} = 3$  ms. Shunting was similar when the polarity of the current waveform was reversed ( $22 \pm 3\%$  of control;  $n = 4$ ).
12. L. Nowak, P. Bregestovski, P. Ascher, A. Herbet, A. Prochiantz, *Nature* **307**, 462 (1984).

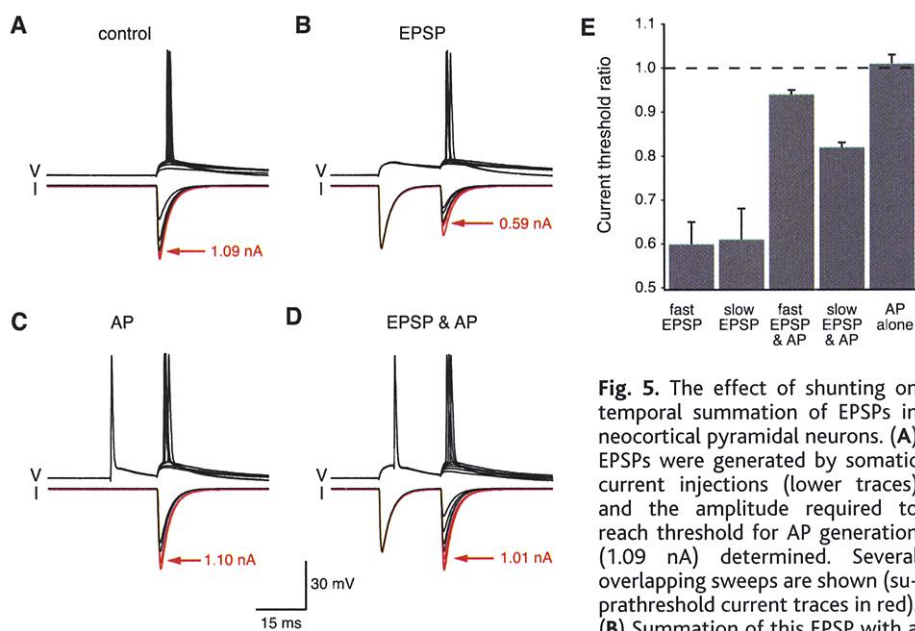


Fig. 5. The effect of shunting on temporal summation of EPSPs in neocortical pyramidal neurons. (A) EPSPs were generated by somatic current injections (lower traces) and the amplitude required to reach threshold for AP generation (1.09 nA) determined. Several overlapping sweeps are shown (suprathreshold current traces in red). (B) Summation of this EPSP with a preceding EPSP (1.0 nA peak amplitude) lowered the current threshold for AP generation (0.59 nA). (C) A preceding antidromic AP timed to occur 5 ms after the first EPSP did not significantly affect the current threshold for AP generation (1.10 nA). (D) When the preceding antidromic AP and EPSP were combined, the current threshold for AP generation (1.01 nA) was similar to that in the absence of the preceding EPSP, suggesting strong shunting of the preceding EPSP. (E) Summary of results from five neurons. The ratio of the current threshold for AP generation with a preceding EPSP, AP or EPSP/AP combination compared to the current threshold without any preceding event. "Fast" EPSPs were generated by current waveforms with  $\tau_{\text{rise}} = 0.3$  ms and  $\tau_{\text{decay}} = 3$  ms [as in (A) to (D)]; "slow" EPSPs were generated by current waveforms with  $\tau_{\text{rise}} = 2$  ms and  $\tau_{\text{decay}} = 20$  ms. The amplitude of the slow EPSP was scaled to produce a similar reduction in AP current threshold as the fast EPSP in the same cell.

amplitude; 20 ms before the control EPSP) lowered the current threshold for AP generation (0.59 nA). (C) A preceding antidromic AP timed to occur 5 ms after the first EPSP did not significantly affect the current threshold for AP generation (1.10 nA). (D) When the preceding antidromic AP and EPSP were combined, the current threshold for AP generation (1.01 nA) was similar to that in the absence of the preceding EPSP, suggesting strong shunting of the preceding EPSP. (E) Summary of results from five neurons. The ratio of the current threshold for AP generation with a preceding EPSP, AP or EPSP/AP combination compared to the current threshold without any preceding event. "Fast" EPSPs were generated by current waveforms with  $\tau_{\text{rise}} = 0.3$  ms and  $\tau_{\text{decay}} = 3$  ms [as in (A) to (D)]; "slow" EPSPs were generated by current waveforms with  $\tau_{\text{rise}} = 2$  ms and  $\tau_{\text{decay}} = 20$  ms. The amplitude of the slow EPSP was scaled to produce a similar reduction in AP current threshold as the fast EPSP in the same cell.

13. M. L. Mayer, G. L. Westbrook, P. B. Guthrie, *Nature* **309**, 261 (1984).
14. G. Stuart, N. Spruston, B. Sakmann, M. Häusser, *Trends Neurosci.* **20**, 125 (1997).
15. P. Fatt, *J. Neurophysiol.* **20**, 61 (1957).
16. These experiments were performed in the presence of ZD7288 (10  $\mu$ M; Tocris, Bristol, UK) to block the effect of the hyperpolarization-activated current  $I_h$  on somatic EPSP time course (22). APs in these experiments were evoked 5 ms after EPSP onset. In control conditions, there was a smaller but still significant difference between shunting of EPSPs generated at distal (>200  $\mu$ m) and at more proximal locations ( $34 \pm 5\%$  versus  $22 \pm 2\%$  of control;  $n = 10$ ;  $P < 0.05$ ).
17. The EPSP shunting was measured before and after application of TTX (1  $\mu$ M) to the dendritic recording site using a puffer pipette. Somatic AP amplitude was unaffected by these applications of TTX ( $-4 \pm 4\%$  change;  $P > 0.05$ ). APs in these experiments were evoked by brief somatic current injections 6 to 7 ms after dendritic EPSP onset.
18. Simulations were performed using NEURON (23) with a time step of 10  $\mu$ s. The single-compartment model consisted of a cylinder 10  $\mu$ m long and 10  $\mu$ m in diameter, with  $C_m = 1 \mu$ F/cm<sup>2</sup>,  $R_m = 12$  k $\Omega$ cm<sup>2</sup> and a passive reversal potential of  $-65$  mV. The synaptic conductance (5 pS) had a reversal potential of 0 mV and exponential rise and decay kinetics, with  $\tau_{rise} = 0.3$  ms and  $\tau_{decay} = 3$  ms.
19. Supplemental Web material is available on Science Online at [www.sciencemag.org/cgi/content/full/291/5501/138/DC1](http://www.sciencemag.org/cgi/content/full/291/5501/138/DC1).
20. D. M. Armstrong, J. A. Rawson, *J. Physiol. (London)* **289**, 425 (1979).
21. G. J. Stuart, H. U. Dodt, B. Sakmann, *Pfluegers Arch.* **423**, 511 (1993).
22. S. R. Williams, G. J. Stuart, *J. Neurophysiol.* **83**, 3177 (2000).
23. M. L. Hines, N. T. Carnevale, *Neural Comput.* **9**, 1179 (1997).
24. M.H. and G.J.S. performed the experiments, analysis, and simulations; G.M. carried out preliminary experiments and simulations describing similar findings in CA1 pyramidal neurons. We thank D. Attwell, B. Clark, M. Farrant, A. Roth, J. Rothman, A. Silver, S. Wang, and S. Williams for comments on the manuscript. We acknowledge support from The Wellcome Trust, the European Community (M.H.), the Human Frontier Science Program (G.J.S.), and Lucent Technologies (G.M.).

25 September 2000; accepted 26 October 2000

## Migration of *Plasmodium* Sporozoites Through Cells Before Infection

Maria M. Mota,<sup>1</sup> Gabriele Pradel,<sup>2</sup> Jerome P. Vanderberg,<sup>2</sup> Julius C. R. Hafalla,<sup>2</sup> Ute Frevert,<sup>2</sup> Ruth S. Nussenzweig,<sup>2</sup> Victor Nussenzweig,<sup>1</sup> Ana Rodriguez<sup>2\*</sup>

Intracellular bacteria and parasites typically invade host cells through the formation of an internalization vacuole around the invading pathogen. *Plasmodium* sporozoites, the infective stage of the malaria parasite transmitted by mosquitoes, have an alternative mechanism to enter cells. We observed breaching of the plasma membrane of the host cell followed by rapid repair. This mode of entry did not result in the formation of a vacuole around the sporozoite, and was followed by exit of the parasite from the host cell. Sporozoites traversed the cytosol of several cells before invading a hepatocyte by formation of a parasitophorous vacuole, in which they developed into the next infective stage. Sporozoite migration through several cells in the mammalian host appears to be essential for the completion of the life cycle.

After *Plasmodium* sporozoites are injected into the mammalian host by mosquitoes, hepatocyte infection is the next obligatory step. In time-lapse video microscopy observations, sporozoites appeared to enter and exit hepatocytes rapidly [(Fig. 1 and Web movie 1) (*I*)] as previously described for macrophages (2). In most cases, hepatocytes survived after parasite entry and exit, but on several occasions cell material was observed leaking into the medium from the site of sporozoite egress, followed by death of the host cell.

To determine whether sporozoites disrupt the hepatocyte plasma membrane while traversing host cells, we used a standard cell wounding and membrane repair assay (3). Wounded cells can be identified by the presence of a cell-impermeant tracer macromolecule within their cytosol, because an open plasma membrane dis-

ruption allows the tracer to enter, after which resealing traps it inside the cell. Dead cells, which do not reseal, are not labeled provided that all exogenous tracer is washed away after membrane disruption. *Plasmodium yoelii* sporozoites, obtained by dissection of infected mosquito salivary glands, were incubated with a mouse hepatoma cell line, Hepa 1-6 (4), in the presence of the cell-impermeant tracer fluorescein isothiocyanate (FITC)-dextran. As a control, Hepa 1-6 cells were incubated with material obtained by dissection of noninfected mosquito salivary glands. After 1 hour, cells were washed to remove all exogenous tracer, then incubated with propidium iodide to detect dead cells. Propidium iodide and dextran-positive cells were found only in cultures incubated with *P. yoelii* sporozoites (Fig. 2A). Endocytosed FITC-dextran was observed as a fine dotted pattern in cell cytosol and was easily distinguished from cytosolic dextran (Fig. 2, A and B). Increasing numbers of Hepa 1-6 cells containing cytosolic dextran were observed up to 1 hour after incubation, remaining constant after this time (Fig. 2C). Sporozoite motility and infectivity are also severely reduced after 1 hour

of incubation. The percentage of dextran-positive cells varied between 10 and 30% in different sporozoite preparations. The percentage of propidium iodide-positive cells reached  $\sim 5\%$ , but the total number of dead cells is probably higher because cells detach from the substrate soon after they die. Flow cytometric analysis (FACS) showed similar percentages of dextran-positive cells and revealed an increase in the size of dextran-positive cells, as described for other cells that have suffered plasma membrane wounding and repair (5).

Wounding of the plasma membrane results in leakage of cytosolic material into the external medium (6). To test whether sporozoites induce release of cytosol from hepatocytes, we incubated *P. yoelii* sporozoites with Hepa 1-6 cells previously loaded with the cytosolic fluorescent marker Green Cell Tracker. *Plasmodium yoelii* sporozoites induced progressive release of this cytosolic marker into the medium (Fig. 2D). These results indicate that sporozoites induce disruption of the host cell membrane, followed by death or survival of the cell, depending on successful resealing of the plasma membrane.

Sporozoites from different *Plasmodium* species, including the human malarial pathogen *Plasmodium falciparum*, displayed similar capacities to induce wounding and repair in Hepa 1-6 cells. Tachyzoites of another apicomplexan parasite, *Toxoplasma gondii*, also infected Hepa 1-6 cells; however, no dextran- or propidium iodide-positive cells were found in the cultures [Web fig. 1 (*I*)]. *Plasmodium* sporozoites induced similar levels of wounding in other types of mammalian cells, such as fibroblast and epithelial cell lines [Web fig. 2 (*I*)].

Sporozoite motility was inhibited by three different mechanisms before incubation with Hepa 1-6 cells to investigate if cell wounding was a result of active penetration of host cells by sporozoites: (i) heat inactivation (7), (ii) incubation with the actin-depolymerizing drug cytochalasin-D (8), and (iii) incubation with a monoclonal antibody (mAb) against *P. yoelii* circumsporozoite protein (anti-CS mAb) (9, 10). All treatments significantly inhibited cell wounding, as measured by a reduction in the

<sup>1</sup>Department of Pathology, <sup>2</sup>Department of Medical and Molecular Parasitology, New York University School of Medicine, 341 East 25 Street, New York, NY 10010, USA.

\*To whom correspondence should be addressed. E-mail: [rodria02@popmail.med.nyu.edu](mailto:rodria02@popmail.med.nyu.edu)